Oppositely Charged Polyelectrolytes. Complex Formation and Effects of Chain Asymmetry

Yoshikatsu Hayashi, Magnus Ullner, and Per Linse*

Physical Chemistry 1, Center for Chemistry and Chemical Engineering, Lund University, P.O. Box 124, S-221 00 Lund, Sweden

Received: April 21, 2004; In Final Form: July 2, 2004

The formation of complexes in solutions of oppositely charged polyions has been studied by Monte Carlo simulations. The amount as well as the length, and thus, the absolute charge of one of the polyions have been varied. There is an increasing tendency to form large clusters as the excess of one kind of polyion decreases. When all polyions have the same length, this tendency reaches a maximum near, but off, equivalent amounts of the two types of polyions. When one kind of polyion is made shorter, the propensity to form large clusters decreases and the fluctuations in cluster charge increases. Simple free-energy expressions have been formulated on the basis of a set of simple rules that help rationalize the observations. By calculating cluster distributions in both grand canonical and canonical ensembles, it has been possible to show the extent of finite-size effects in the simulations.

Introduction

Solutions containing both positively and negatively charged polyions (in the following referred to as polycations and polyanions, respectively) have gained interest recently. The strong Coulomb interaction between the oppositely charged polyions leads to a strong association. This association often initiates an associative phase separation, resulting in one polymer-rich and one polymer-poor phase.

Kabanov and co-workers[1−5] have carried out comprehensive studies of soluble polyion complexes including the preparation conditions of the complexes, their structure and kinetics, and exchange reactions between polyion complexes and other polyions as a function of polyion properties and salt concentration. Pogodina and Tsvetkov[6] have studied the formation of complexes in solutions of oppositely charged polyelectrolytes over a wide range of mixing ratios. At a specific mixing ratio, they observed a simultaneous increase in mass, size, and polymer density of the polyion complexes formed. Finally, the formation of alternating layers of polycations and polyanions at solid surfaces,[7,8] originally developed by Decher and co-workers, is another and rapidly expanding area that involves mixtures of polyions.[9]

To elucidate the general tendencies of the influence of salt on polyelectrolyte complex formation, Dautzenberg[10] studied this process by static light scattering as a function of the ionic strength of the medium and the molar ratio of the solution components. He reported that in most systems the internal structure of the complexes is marginally affected by salt. However, he also concluded that a prediction of the effects of salt during complex formation is very difficult, because the process depends on the specific characteristics of the polyelectrolyte components.

In simulation studies, flexible polyions are normally modeled as linear chains of charged beads in a dielectric continuum. Simple ions are either included explicitly or implicitly using a screened Coulomb potential as an effective interaction between chain beads. Christos and Carnie[11] have simulated polyelectrolyte solutions in the presence of added salt using the screened Coulomb potential. Later, Stevens and Kremer presented a series of investigations of salt-free polyelectrolyte solutions with explicit ions[12−14] and made comparisons with a screened Coulomb potential.[15] Such comparisons have also been made on the basis of simulations of single chains.[16−19]

As for systems of oppositely charged polyelectrolytes, Borue and Erukhimovich[20] have presented a statistical theory for polyelectrolyte complexes in a stoichiometric solution and have calculated internal properties such as monomer density as functions of salt concentration and solvent quality. Furthermore, Srivastava and Muthukumar[21] have examined the structure formed by two flexible and oppositely charged polyelectrolytes of the same length and absolute charge at different lengths and charges. They found a considerable reduction of the chain extensions upon complex formation and reported on scaling exponents for the radius of gyration. Moreover, Winkler et al.[22] have investigated essentially the same system as a function of the interaction strength between the chain beads and reported on scaling exponents as well as on very compact structures and pronounced local order at high interaction strength. Dias et al.[23] have presented a series of simulations of one chain with 120 charged beads and shorter oppositely charged chains of varying length and number. They discussed the conditions leading to compactation of the long chain and the nature of aggregates formed. Recently, Messina et al.[24,25] have simulated the formation of polyelectrolyte multilayering at charged surfaces of different geometries. A nonelectrostatic short-range interaction between the charged surface and the polyions was needed to establish a multilayer; without that interaction, the formation of complexes in bulk strongly competed with the adsorption of the polyions onto the charged surface.

Our aim is to improve our understanding of the complex formation in solutions of oppositely charged polyions based on coarse-grained models. In our first contribution,[26] we investigated the properties of solutions of polycations with different amounts of polyanions up to 50% charge equivalence with the two types of polyions having the same absolute charge. Two models were used: one involving only polyions with the beads interacting via a screened Coulomb potential and another where explicit simple ions were included and all charges interacted

10.1021/jp048267y CCC: $27.50
Published on Web 08/28/2004

through a Coulomb potential. We concluded that the two models provided qualitatively the same results, and for polyion conformations within a complex, the agreement was even quantitative.

In our second contribution,[27] we extend our study to compositions of the two polyions up to equivalent amounts of charges on polycations and polyanions. We found that the strongest tendency to form large complexes appeared slightly before equivalent amounts, whereas at equivalent amounts the large clusters were partly broken up. Much of our results was condensed into four simple rules: (I) coexistence of oppositely charged clusters is avoided to gain favorable electrostatic potential energy; (II) the cluster net charge density (cluster net charge divided by cluster size) is minimized to reduce the electrostatic repulsion among excess charges; (III) the total net charge (the number of excess polyions in a cluster) is kept low for the same reason; and (IV) the number of clusters is maximized to gain translational entropy. In this context, an uncomplexed (referred to as free) polyion is also treated as a cluster. We also pointed out that the reduction in cluster size for the charge equivalent system was an effect of having monodisperse polyions with perfect symmetry between polycations and polyanions. This corresponds to an ideal case, which would be difficult to realize at experimental conditions, at least with synthetic polymers. We found that larger clusters were promoted in systems containing (i) monodisperse polycations and polyanions with slightly different absolute charges or (ii) polydisperse polyions with the same chain distributions for polycations and polyanions.

In this contribution, we extend our study of systems containing oppositely charged polyions (i) to larger system size, (ii) to include systems where polycations and polyanions have different absolute charges, and (iii) to involve a theoretical analysis based on a simple free-energy model. Regarding systems with equal absolute charges, the use of a larger system size leads to a modification of our previous conclusions.[27] In more detail, we found it fruitful to introduce a cluster surface energy to rationalize our new observations and to reexpress the electrostatic effect as a dependence on surface charge, which combines the previous rules II and III. As the difference of the absolute charge of polycations and polyanions increases, the nature of the complexes formed differs. In particular, as the short polyions become shorter than a 10-mer, the tendency of forming a large cluster at equivalent amounts disappears.

The outline of this paper is as follows: After the Introduction, we describe the model and some simulation aspects. In the following section, we report on the formation of polyion complexes as a function of the polyion composition and chain length observed through structure factors and cluster size distributions. Our empirical rules are expressed in a quantitative form, and finite-size effects in different ensembles are discussed with the help of simple free-energy calculations in the next section, which is followed by conclusions. Finally, the parametrization and other details of the free-energy expressions are discussed in an appendix.

Model and Methods

Model. As in our previous studies,[26,27] the polyelectrolyte solutions, containing charged polyions and simple ions in an aqueous medium, is represented by a coarse-grained model. The polyions are described as freely jointed chains with charged hard spheres (beads) connected by harmonic bonds. The electrostatic interaction is represented by a screened Coulomb potential, which treats the simple ions and the solvent implicitly. Previously, we found that a screened Coulomb potential provides a reasonable description of the effects of the simple ions.[26]

The total interaction energy U of the system is pairwise additive. There are two main contributions arising from nonbonding and bonding interaction potentials according to

$$U = \sum_{i<j}^{n_{pos}+n_{neg}} u_{nonbond,ij} + \sum_{m=1}^{N_{pos}+N_{neg}} \sum_{i=1}^{N_{bead,m}-1} u_{bond,m,i} \quad (1)$$

where n_{pos} and n_{neg} denote the total number of positive and negative beads, respectively, N_{pos} and N_{neg} are the number of polycations and polyanions, respectively, and $N_{bead,m}$ is the number of beads in chain m.

The nonbonding potential $u_{nonbond,ij}$ for a pair ij, where i and j are any two beads, is given by

$$u_{nonbond,ij}(r_{ij}) = \begin{cases} \infty & r_{ij} < R_i + R_j \\ z_i z_j k_B T l_B \dfrac{\exp(-\kappa r_{ij})}{r_{ij}} & r_{ij} \geq R_i + R_j \end{cases} \quad (2)$$

where z_i is the valence of bead i, k_B Boltzmann's constant, T the temperature, R_i the radius of bead i, and r_{ij} the distance between beads i and j. The Bjerrum length is defined as

$$l_B = \frac{e^2}{4\pi\epsilon_0\epsilon_r k_B T} \quad (3)$$

with e being the elementary charge, ϵ_0 the permittivity of vacuum, and ϵ_r the relative permittivity of the solvent. In eq 2, κ denotes the inverse Debye screening length given by

$$\kappa^2 = 4\pi l_B \sum_k z_k^2 \rho_k \quad (4)$$

where the summation extends over the implicit simple ions (monovalent counterions of the polyions) with ρ_k denoting the number density of simple ions of type k.

The bond potential $u_{bond,m,i}$ between beads i and $i+1$ belonging to polyion m is given by the harmonic potential

$$u_{bond,m,i} = \frac{k_{bond}}{2}(r_{m;i,i+1} - r_0)^2 \quad (5)$$

where r_0 is the equilibrium bond length, k_{bond} the force constant, and $r_{m;i,i+1}$ the distance between beads i and $i+1$ of polyion m.

Monovalent beads ($z_i = 1$) with a radius $R_i = 2$ Å were used throughout. All systems were considered at $T = 298$ K using $\epsilon_r = 78.4$, representing water as the solvent ($l_B = 7.15$ Å). The bond parameters $r_0 = 5$ Å and $k_{bond} = 0.4$ N/m were used, and with the other interactions included, the root-mean-square (rms) bead-to-bead separation became ≈5.9 Å.

Two sets of systems have been considered, viz, polycations and polyanions of (i) equal and (ii) unequal chain lengths. In the first set, the number of beads in the polycations and the polyanions are the same and fixed to $N_{bead} = 20$. Systems containing $N_{pos} = 20$ polycations and $N_{neg} = 0-20$ polyanions are considered, and they will be referred to as system 0 to system 20. Table 1 provides an overview of the systems, including the screening length κ^{-1}.

In the second set, systems containing polycations and polyanions of unequal length and hence of unequal absolute charge are considered. For convenience, the polyions will be referred to as long and short ones with in total n_{long} and n_{short} beads, respectively, in the system. We focus on three cases of

TABLE 1: Overview of the Systems with Equal Chain Lengths[a]

label	N_{pos}	N_{neg}	κ^{-1}/Å	$\langle \Delta \mathbf{r}_{neg}^2 \rangle^{1/2}$/Å[b]
system 0	20	0	14.9	
system 10	20	10	12.2	550
system 15	20	15	11.3	480
system 16	20	16	11.1	490
system 17	20	17	11.0	510
system 18	20	18	10.8	420
system 19	20	19	10.7	390
system 20	20	20	10.6	500

[a] $N_{bead} = 20$. [b] Root-mean-square displacement for negatively charged beads during the production simulation.

TABLE 2: Overview of the Systems with Unequal Chain Lengths[a]

			stoichiometric conditions					
			excess of long chains		equivalent amounts		excess of short chains	
r_{length}	$N_{bead,long}$	$N_{bead,short}$	N_{long}	N_{short}	N_{long}	N_{short}	N_{long}	N_{short}
2	40	20	10	10	10	20	5	20
4	40	10	10	20	10	40	5	40
8	40	5	10	40	10	80	5	80

[a] $r_{length} = N_{bead,long}/N_{bead,short}$ denotes the chain-length ratio, $N_{bead,long}$ is the number of beads in a long chain, $N_{bead,short}$ is the number of beads in a short chain, N_{long} is the number of long chains, and N_{short} is the number of short chains. The smallest root-mean-square displacement for beads in the long chains during the production simulation was 180 Å and appeared for $r_{length} = 2$ and equivalent amounts.

asymmetry, viz, $r_{length} \equiv N_{bead,long}/N_{bead,short} = 2$, 4, and 8 with the longer chain containing $N_{bead,long} = 40$ beads. Three different stoichiometric conditions are considered: (i) an equal number of beads and absolute charges residing in long and short chains, $n_{long} = n_{short}$; (ii) a 2-fold stoichiometric excess of the short chains, $n_{short} = 2n_{long}$; and (iii) a 2-fold stoichiometric excess of the long chains, $n_{long} = 2n_{short}$. Table 2 provides an overview of these systems investigated.

Method. The equilibrium properties of the model systems were obtained by performing canonical Monte Carlo simulations according to the Metropolis algorithm,[28,29] using the simulation package MOLSIM.[30] The polyions were enclosed in a cubic box with a box length $L_{box} = 200$ Å, and periodic boundary conditions were applied. A spherical cutoff at 80 Å was employed for the screened Coulomb interactions.

Due to the strong complexation between oppositely charged polyions, the selection of trial moves is important for adequate sampling and an examination of the convergence of the simulation is required. The chains were initially placed randomly in the simulation box. The equilibrations involved 3×10^5 passes (trial moves per bead), and the production runs were 9×10^5 passes. The polyions were subjected to four types of trial displacements, viz, (i) translation of a single bead, (ii) slithering move, (iii) pivot rotation, and (iv) translation of an entire chain. The selection among the four different trial moves was made randomly using the weights 0.4, 0.3, 0.1, and 0.2, respectively.

Our simulation protocol leads to bead rms displacements for beads located in complexed polyions of at least 390 Å in the most demanding case with equal chain lengths (see Table 1) and about half of that for the case of the strongest complexation with unequal chain lengths (see Table 2), the latter being smaller because the beads are located in longer chains. Hence, the rms displacements are at least of the same length as the system size and are hence satisfactory. Further details on the protocol and convergence of simulations of these systems have previously been given.[26]

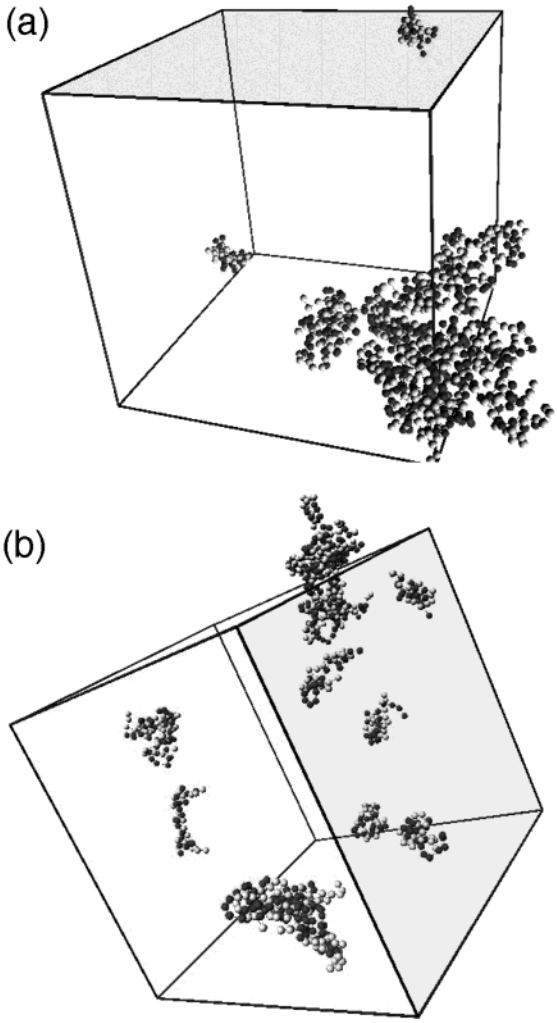

Figure 1. Final configurations of (a) system 18 and (b) system 20. The systems contain 20 polycations composed of 20 positively charged beads (light gray spheres) and 18 and 20 polyanions, respectively, composed of 20 negatively charged beads (dark gray spheres). Some beads have been translated in accord with the periodic boundary conditions (one box length) to better illustrate the complex formation. The simulation boxes have been rotated to give a clear view in each case.

Simulation Results

Equal Chain Length. *Overview.* Not unexpectedly, complexes consisting of polycations and polyanions are formed when both are present in the solution. As an illustration, Figure 1 displays the final configurations of systems 18 and 20. In the former case with $N_{pos} = 20$ polycations and $N_{neg} = 18$ polyanions, three complexes are present, one containing 18 polycations and 16 polyanions and another two complexes made up of the remaining two pairs of polyions of opposite charge (Figure 1a). With equal numbers of polycations and polyanions, several complexes of different sizes are observed (Figure 1b), and all of them are neutral. Thus, pronounced complexation in solutions containing oppositely charged polyions appears when the solution is near or at equivalent amounts.

Solution Structure. The spatial inhomogeneity of the solution can be quantified by structure factors. In particular, the partial structure factor $S_{pos}(q)$ involving the positively charged beads will be used to examine the change of the solution structure as

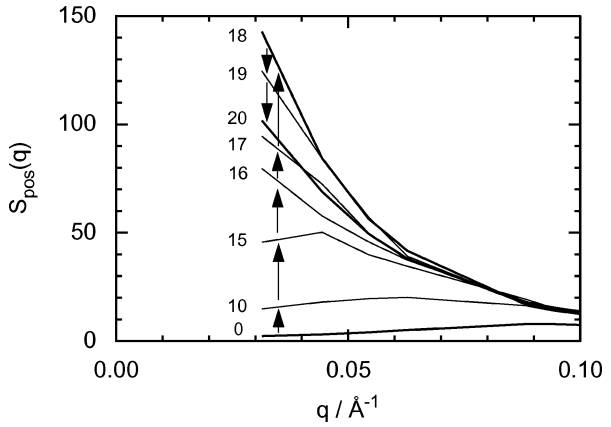

Figure 2. Partial structure factors of positive beads $S_{pos}(q)$ for the indicated systems. The arrows show the order of increasing amounts of polyanions.

polyanions are added. Here, $S_{pos}(q)$ was directly evaluated from its definition

$$S_{pos}(q) \equiv \left\langle \frac{1}{n_{pos}} \left| \sum_{j=1}^{n_{pos}} \exp(i\mathbf{q}\cdot\mathbf{r}_j) \right|^2 \right\rangle \tag{6}$$

where $\mathbf{q}$ is the wave vector with magnitude q, $\mathbf{r}_j$ the position of positive bead j, and $\langle ... \rangle$ denotes an ensemble average. It should be noted that the lower limit, q_{low}, of the wave vector is controlled by the box size according to $q_{low} = 2\pi/L_{box}$ ($\approx$0.031 Å^{-1}).

Figure 2 displays $S_{pos}(q)$, and we focus on small wave vectors to examine the structures appearing at large length scales. At q close to q_{low}, the general trend is that $S_{pos}(q)$ grows, reaches a maximum, and decreases as the number of polyanions is increased. The growth of the structure factor at small q implies increased long-ranged spatial correlations among the positive beads appearing in clusters with increasing number of positively charged beads.

On closer inspection, the structure factor of system 0 containing only $N_{pos} = 20$ polycations display a weak maximum at $q \approx 0.08$ Å^{-1} (barely visible with the scales selected), indicating that the polyions are well separated in a solution of only polycations. The structure factor of system 10, which contains $N_{neg} = 10$ polyanions, has a larger magnitude at small wave vectors and displays a maximum shifted to $q \approx 0.06$ Å^{-1}. This trend of larger magnitude and a maximum shifted to smaller q is continued in system 15. The growth of the maximum as N_{neg} is increased describes a larger number of positively charged beads located in complexes, and the shift to smaller q indicates a larger average separation between the collections of the positive beads.

Upon further addition of polyanions, the general trend is that $S_{pos}(q)$ continues to grow at small q, *but* the largest amplitude now appears at q_{low}. The largest amplitude of $S_{pos}(q_{low})$ appears for $N_{neg} = 18$. This growth and the absence of a maximum are consistent with the formation of a large complex comprising most of the polyions (Figure 1a).

Beyond $N_{neg} = 18$, the partial structure factor for the positive beads at low wave vectors starts to decline. The difference in magnitude of q_{low} at $N_{neg} = 18$ and 19 is close to not being statistically significant, but it is clear that there is a maximum between systems 17 and 20. The reduced partial structure factor for system 20 is hinted at in the snapshots of Figure 1 as the breakup of the large complex appearing for system 18 into several smaller ones for system 20. A more detailed picture is given by the cluster distributions in the next section.

Cluster Composition. The formation of various complexes at different conditions has been investigated by calculating the number of clusters containing different numbers of polycations and polyanions. Two polyions are considered to belong to the same cluster if they are "connected" directly or indirectly through one or several other polyions. Two polyions are directly connected if their center-of-mass separation does not exceed 30 Å. From the simulations, the cluster size probability distribution $P_{m,n}$ was calculated according to

$$P_{m,n} = \frac{(m+n)\langle N_{m,n}^{cluster} \rangle}{\sum_{m,n} (m+n)\langle N_{m,n}^{cluster} \rangle} \tag{7}$$

where $\langle N_{m,n}^{cluster} \rangle$ is the average number of clusters containing m polycations and n polyanions and the denominator is equal to $N_{pos} + N_{neg}$ by chain conservation. Note that $P_{m,n}$ is a "mass"-weighted measure of the cluster size distribution, where the *number* of chains $m + n$ in a cluster provides the weight. It represents the probability that any polyion, chosen randomly among both polycations and polyanions, will be found in a cluster of type m:n. In other words, it shows how the polyions are distributed between different clusters. When $m + n = 1$, the single chain constituting the cluster is referred to as a free chain.

Figure 3 shows the distribution of $P_{m,n}$ as a function of m and n for systems 10, 18, 19, and 20. In system 10 with a 2-fold excess of the polycations, the 2:1 cluster is by far the dominating one. Some 3:2 clusters appear as well, but with only a small probability (Figure 3a).

System 18 contains an excess of two polycations. The clusters appearing in Figure 3b can conveniently be divived into three classes: neutral clusters ($m = n$), charged clusters with an excess of one polycation ($m = n + 1$), and charged clusters with an excess of two polycations ($m = n + 2$). The distribution of neutral clusters displays a maximum for the 1:1 cluster and decreases continuously as the total number of polyions in the clusters increases. The distribution of clusters with an excess of one polycation is broad and displays a maximum for the 9:8 cluster, whereas the distribution of clusters with an excess of two polycations has a maxium for the 17:15 cluster. Hence, for the charged clusters, the most probable size increases with the number of excess polycations.

The cluster size distribution for system 19 (Figure 3c) resembles that of system 18. However, the probability of neutral clusters is increased; there is a larger probability for the 1:1 cluster as well as larger neutral clusters. The probability distribution of clusters with an excess of one polycation is very broad and its maximum is displaced to the 18:17 cluster.

Finally, in system 20, containing equal amounts of polycations and polyanions, only neutral clusters are present (Figure 3d). A *bimodal* distribution of neutral clusters appears with maxima at 1:1 and 15:15 clusters. Hence, small and large neutral clusters coexist. In our previous study with a smaller system containing 10 polycations and 10 polyanions,[27] only a continuously decaying probability with increasing cluster size was observed.

The distribution of cluster compositions can be rationalized by four simple rules. They are (I) coexistence of oppositely charged clusters is avoided to gain favorable electrostatic potential energy, (II) the cluster surface charge density (or rather the cluster net charge squared divided by the surface area) is

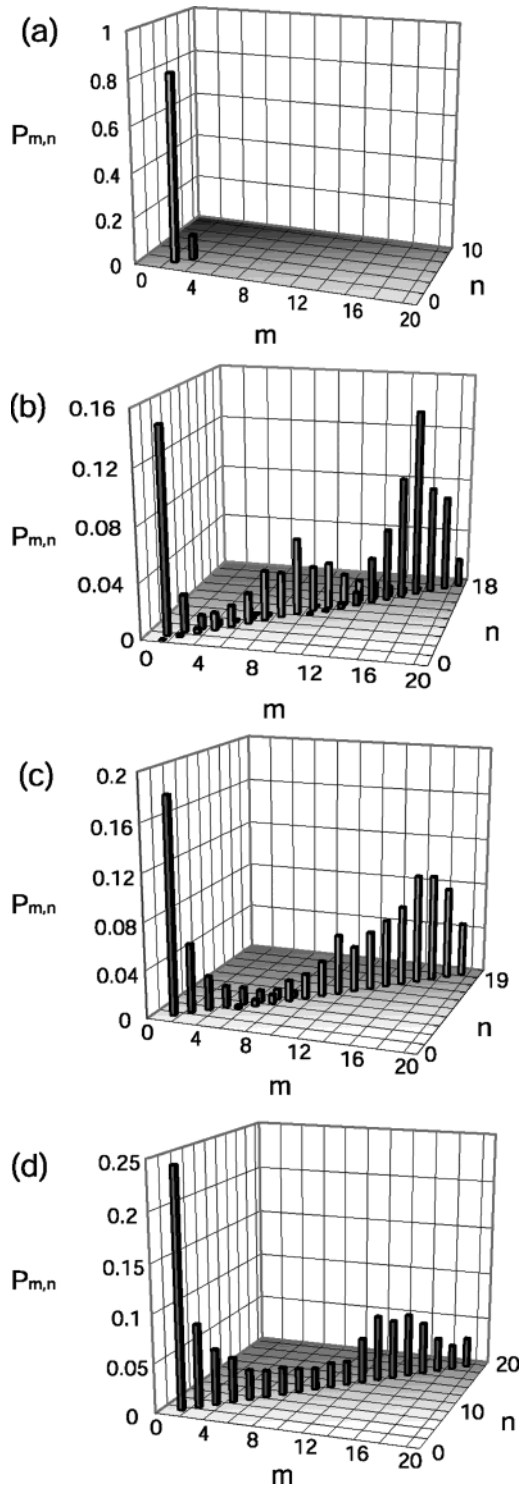

Figure 3. Cluster size probability distribution $P_{m,n}$ vs the number of polycations m and the number of polyanions n in polyion complexes for (a) system 10, (b) system 18, (c) system 19, and (d) system 20. Dark gray columns represent neutral clusters, light gray columns charged clusters with $m = n + 1$, and black columns charged clusters with $m = n + 2$.

minimized to reduce the electrostatic repulsion among excess charges, (III) the total area of cluster surfaces is minimized to reduce the loss of electrostatic correlation energy, and (IV) the number of clusters is maximized to gain translational entropy.

As compared to our previous set of rules, given in the Introduction, the old rules II and III have been combined into one new rule II, which considers the surface charge density instead of the volume charge density. The old rule III (minimized net charge) was based on the observation that 2:1 clusters are promoted at the expense of 4:2 clusters when the strength of the interactions is increased. The two types of clusters have similar volume charge densities (the same number of charges per polyion in the cluster), and the old rule II did not present an energetic contribution to favor the smaller cluster, but because the surface area grows slower with respect to the number of polyions in a cluster than the volume, the new rule II does and accommodates the earlier observation. Furthermore, a completely new rule III has been introduced.

Rule I limits the range of cluster types to include neutral clusters and charged clusters with at most the same excess as the total system. Rule II promotes clusters with the same composition as the solution and only one excess polyion, which means that it allows the excess polyions to collect neutral pairs to form larger clusters but can also split large clusters with more than one excess polyion; i.e., it prescribes separating the excess charges and dividing the neutral pairs among them. Rule III opposes small clusters, and rule IV favors a large number of clusters. Hence, assuming that rule I is satisfied, large clusters are always energetically favored by rule III and entropically disfavored by rule IV, whereas rule II is allied with a sliding scale of sizes depending on the amount of excess polyion charge. These rules will be expressed in a more quantitative form in the section about free-energy calculations.

The simulations have been performed in canonical ensembles with a fixed number of polyions, which imposes additional constraints, because only certain combinations of clusters are allowed. One effect is that when the energetic components that favor large clusters are not very large, the largest clusters are suppressed, because there are many more combinations with small clusters. This will also be discussed in the free-energy section.

Regarding system 10, the dominance of 2:1 clusters can be viewed as a balance of the rules as follows. Separate 1:0 and 1:1 clusters would be favored by rule IV but violates rule II, obviously rule II takes precedence over rule IV. Moreover, the merging of, e.g., two 2:1 clusters to a 4:2 cluster, which would be promoted by rule III, is depressed by rule II and rule IV jointly.

An intriguing question is how the two excess polycations are distributed among the clusters in system 18. Besides the appearance of neutral clusters, rule II would favor the presence of two clusters, each with one excess polycation. However, a large fraction of the clusters contains two excess polycations; hence at cluster sizes involving ca. 30 polyions the importance of rule II is challenged by rule III. Therefore, at sufficiently large area, a cluster can sustain more than one excess polycation. In addition to charged clusters, the considerable number of neutral clusters is promoted by rule IV.

Finally, the appearance of only neutral clusters for equivalent amounts of polycations and polyanions shows that rule I describes the system well. The appearance of large neutral clusters is here attributed to rule III; the merging of several small clusters leads to a smaller total cluster area. However, as for systems 18 and 19, rule IV promotes a considerable fraction of small clusters, which for energetic reasons are neutral. The lack of very large clusters is an effect of the canonical constraints.

The introduction of rule III containing a surface free energy appears to be the simplest way of explaining (i) the bimodal cluster size distribution for systems containing equivalent amounts of polycations and polyanions and (ii) the existence of clusters having an excess of two polycations in system 18.

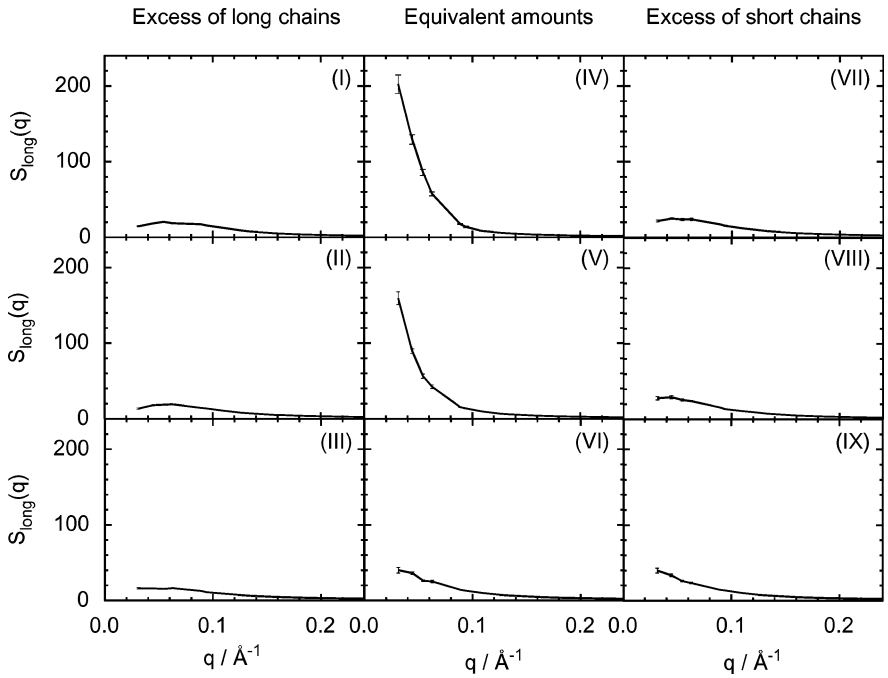

Figure 4. Partial structure factors of positive beads $S_{pos}(q)$ at length ratio $r_{length} = 2$ (upper row), 4 (central row), and 8 (lower row) for a 2-fold excess of long chains (left column), equivalent amounts (central column), and a 2-fold excess of short chains (right column).

The physical origin of the surface term arises from the fact that the electrostatic free energy of an electroneutral system is negative because the neighborhood of a cation contains, on average, more anions than cations and vice versa. However, this attractive correlation free energy becomes smaller in magnitude for charges near a surface, hence the electrostatic correlation is less favorable when the surface area is large and tends to minimize the total area.

Unequal Chain Length. The propensity to form clusters when the polyanions and polycations are of unequal chain length (and unequal absolute charge) will now be considered. Three different stoichiometric conditions, each for three different chain-length ratios, have been examined, making a total of nine cases (see Table 2). The discussion will start with equivalent amounts of total charge on long chains and on short chains followed by, in turn, an excess of long chains and an excess of short chains. For each stoichiometric condition, we will start with the smallest chain-length ratio.

Solution Structure. The partial structure factors $S_{long}(q)$ based on the charged beads residing in the long chains have been calculated to characterize the solution structure and are shown in Figure 4. For identification, each panel is labeled with a Roman numeral.

In the case of equivalent amounts and with the short chains being 20-mers (panel IV) or 10-mers (panel V), $S_{long}(q)$ increases dramatically as q approaches q_{low} from above. Again this is a signature of the existence of spatial correlations appearing on a length scale of $2\pi/q_{low}$ consistent with the formation of large clusters. With 5-mers as short chains (panel VI), the growth of $S_{long}(q)$ at decreasing q is much less pronounced, indicating a much weaker tendency to form large clusters.

We now consider the situation with an excess of long chains. Independent of the length ratio (panels I, II, and III), the partial structure factors display only a moderate magnitude ($\approx$20) at low q and moreover a weak maximum at $q \approx 0.05-0.06$ Å^{-1}. Hence, the solution is composed of fairly small repelling entities with a center-to-center separation of about 110 Å.

For the systems with an excess of short chains (panels VII, VIII, and IX), the solution structures resemble those with an excess of long chains. One difference, however, is a ca. 50% higher magnitude at small wave vectors and the absence of a maximum for the case with 5-mers (panel IX). Despite the appearance of slightly larger polyion entities, there is no sign of aggregation on a grand scale, as in panels IV and V.

Cluster Composition. The cluster-size probability distributions $P_{m,n}$ of the different cases of unequal chain lengths are provided in Figure 5 with m and n now referring to short and long chains, respectively. The layout of Figure 5 is the same as that of Figure 4.

Equivalent Amounts. Panel IV of Figure 5 shows $P_{m,n}$ for the case with the chain-length ratio $r_{length} = 2$. Significant probabilities are only found along the "diagonal" $m = r_{length}n$, demonstrating that neutral clusters are formed almost exclusively; i.e., the composition of the clusters is the same as that for the solution. There is a small amount of small clusters (mainly 2:1), but the solution is dominated by large clusters (mainly 20:10, 18:9, and 16:8). The probability for neutral clusters of intermediate size is small and essentially no free polyions are present. Compared to system 20, we have connected pairs of 20-mers of one kind into 40-mers, thereby reducing the entropic penalty for forming large clusters. Furthermore, the electrostatic repulsion between the two halves of a 40-mer cannot be removed by separating two 20-mers as in system 20. Thus, the scales have been clearly shifted in favor of large clusters as we can see by comparing Figure 3d with panel IV of Figure 5.

When the 20-mers are replaced by 10-mers giving a chain-length ratio $r_{length} = 4$, panel V, the cluster size distribution is somewhat changed. Again the probability along the diagonal $m = r_{length}n$ dominates, but small fluctuations about that diagonal appear, indicating the appearance of charged complexes beside the neutral ones. A skewed bimodal distribution along the diagonal remains, but the probability of the largest cluster is reduced and complexes with intermediate sizes are slightly more abundant. There is a small probability of finding free 10-mers, consistent with the observation that undercharged

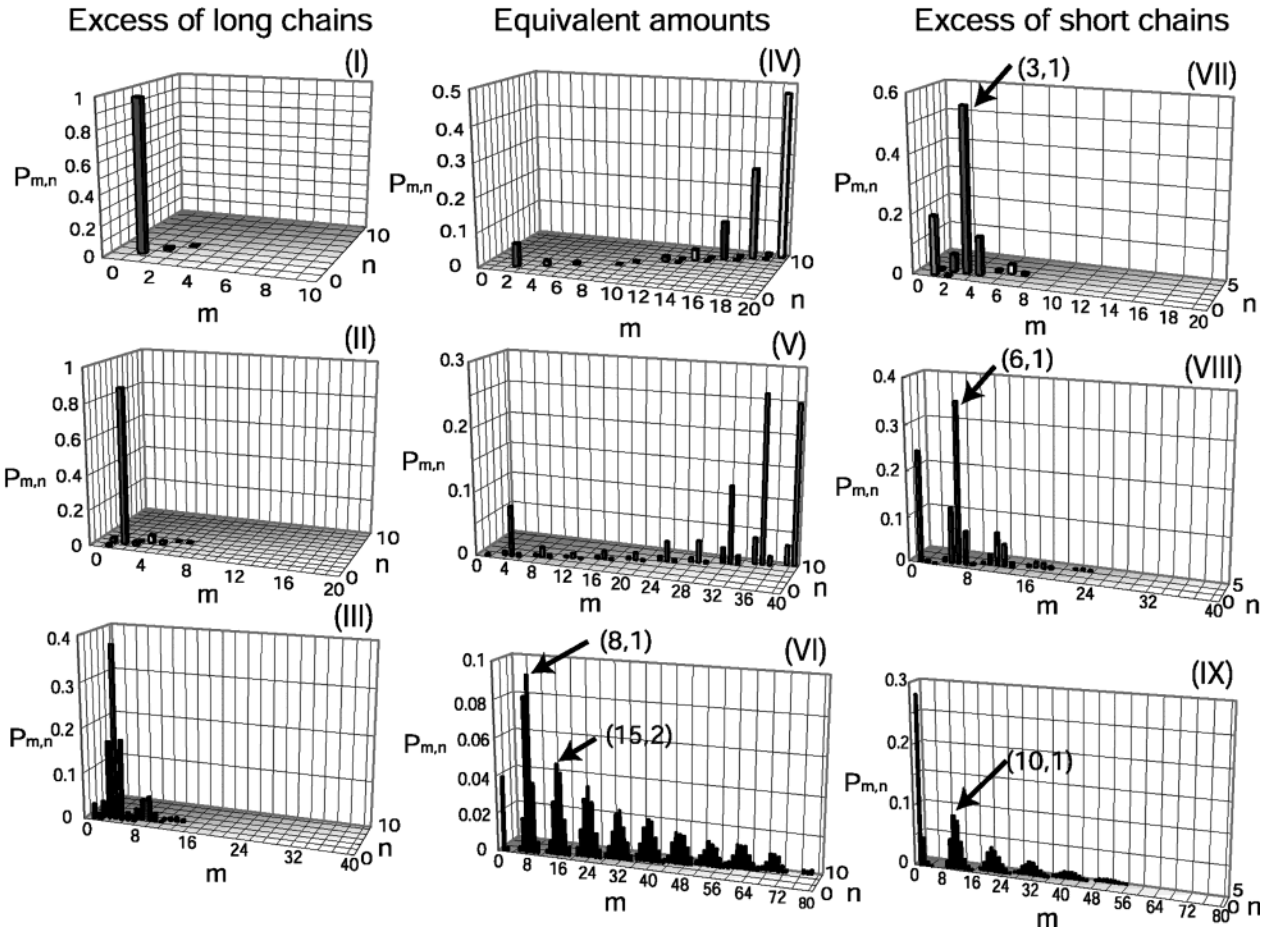

Figure 5. Cluster size probability distribution $P_{m,n}$ vs the number of short chains m and the number of long chains n at length ratio $r_{length} = 2$ (upper row), 4 (central row), and 8 (lower row) for a 2-fold excess of long chains (left column), equivalent amounts (central column), and a 2-fold excess of short chains (right column).

complexes ($m < r_{length}n$) are more probable than overcharged ones ($m > r_{length}n$).

When the length of the short chains is halved again, now to 5-mers, which leads to $r_{length} = 8$, the cluster size distribution is strongly affected (panel VI). There are large fluctuations around the diagonal $m = r_{length}n$, showing a considerable variation in the net charge of the complexes. The probabilities are higher for undercharged complexes (same sign of the charge as the long polyions) than for the corresponding overcharged ones, and the distributions even show maxima for undercharged clusters when these contain more than one long chain. Second, the probabilities along the diagonal decay continuously as the number of large chains in a complex is increased. Thus, the short chains are not any longer able to electrostatically "glue" the long chains together into large clusters. Panel VI also shows the presence of a considerable fraction of free 5-mers. In this case we have increased the available entropy further, and each short chain has less to gain from the electrostatic correlation attraction. The system would therefore, on average, prefer to not neutralize the 40-mers completely and retain free short chains and charged clusters.

In the limit that we cut up the short chains completely, we would just have a solution of polyions and monovalent counterions, as in system 0. In this case, we would have well-separated polyions with counterions forming diffuse double layers around them.

A similar trend has been seen by Dias et al.,[23] who noted that at least 5-mers were required for the compaction of an oppositely charged 120-mer at equivalent amounts and that a tighter complex was formed when the short chains were longer.

Excess of Long Chains. We now consider the case with a 2-fold excess of long chains. Panel I shows that for an equal number of long and short chains, at the chain-length ratio $r_{length} = 2$, essentially only 1:1, i.e., undercharged, complexes are formed. The minute fractions of larger clusters are restricted to multiples of 1:1 clusters.

With 10-mers as short chains and $r_{length} = 4$, panel II shows that mainly 2:1 and still undercharged complexes are present. However, small probabilities of 1:1 and 3:1 complexes also appear as do free short chains.

The corresponding cluster size distribution for 5-mers as short chains is presented in panel III. Now, considerable fluctuations in the number of short chains occur around the 4:1 complex, which is equal to the solution stoichiometry. There is also a small probability of complexes possessing two long chains with a variable number of short chains.

Excess of Short Chains. Finally, the situation where an excess of short chains is present will be discussed. First, panel VII displays the results for $r_{length} = 2$. As for the excess of long chains, complexes with essentially only one long chain are formed. The largest probability appears for a 3:1, and hence overcharged, complex. There is also a considerable fraction of free 20-mers.

Panel VIII shows that, as the length of the short chains is reduced, the decay of the probability along the diagonal becomes more gradual; i.e., complexes with two long chains become more

likely. As with 20-mers, the complexes are overcharged, the most likely overcharge being 50% and 40% for complexes with one and two long chains, respectively. The fraction of free 10-mers is large.

Finally, with an excess of 5-mers as short chains, the probability is increasing for complexes with two and three long chains. There is a considerable fluctuation in the number of short chains in a complex. As with 20-mers and 10-mers, the complexes are overcharged, but the overcharge is reduced to ca. 25%, although in numbers, it still means two extra short chains for each long. Again the fraction of free short chains is large. There is even a significant probability for 2:0 clusters, i.e., clusters of two short chains, which suggests that with a distributed solution of many short chains, our definition of a cluster with a maximum center-of-mass distance of 30 Å, is too wide.

Varying Stoichiometric Conditions. Now, let us briefly consider the main findings for unequal chain lengths from the point of view of varying the stoichiometric condition at fixed length asymmetry on the basis of the results from the partial structure factors and the cluster size analysis.

A dilute solution of only long polyions (40-mers) is characterized by well-separated polyions originating from their repulsive Coulomb interaction (similar to that of 20-mers shown in Figure 2). Upon addition of shorter and oppositely charged polyions, complexes between the oppositely charged polyions are formed. At a 2-fold excess of the long polyions, the attractive Coulomb interaction between the oppositely charged polyions leads to the formation of complexes containing one long polyion and several short polyions with a charge ratio corresponding to the solution stoichiometry (panels I−III of Figure 5). The complexes stay well separated owing to their net charge (panels I−III of Figure 4).

At equivalent amounts, the behavior of the solution depends strongly on the length of the short polyions. With 20-mers or 10-mers, neutral complexes are formed with a dominance of very large clusters (panels IV and V of Figures 4 and 5). With an excess of short chains, the large complexes are broken up and the long chains are again dissolved into a homogeneous solution containing small complexes, now consisting essentially of one long chain and several short ones (panels VII and VIII of Figures 4 and 5).

However, when the short chains are 5-mers, even at equivalent amounts, the complexes contain mostly only a few long chains (panels VI of Figure 5). This is understood from the fact that the electrostatic energy of binding the small chains to the larger ones decreases per chain; hence the enthalpy−entropy balance eventually favors free small chains as their size is reduced. In the limit when the small polyions become monomers we approach the condition of a solution containing one type of polyion and simple ions, a solution characterized by individual polyions with most of their counterions separated from them.

When there is an excess of short chains, many of them are free and the average net charge of the clusters is lower than in an excess of long chains with the inverse ratio of total charges on long and short chains (panels VII−IX compared to panels I−III of Figures 4 and 5).

Free-Energy Calculations

The simulations give detailed cluster distributions and these can be rationalized with the help of the simple rules, but to get more insight into the balance between different effects, we need to quantify them. Furthermore, the simulations are performed in canonical ensembles with fixed numbers of polyions, which restricts the possible combinations of clusters. In a macroscopic system, all types of clusters can exist simultaneously at various concentrations, as long as the clusters do not reach macroscopic size, which would correspond to a phase separation. The constraints of a canonical ensemble can be released by considering a grand canonical ensemble, where the chemical potentials of the polyions are fixed instead of their numbers. We will set up simple expressions to describe the system in a manner closely related to the qualitative rules and calculate cluster distributions in both canonical and grand canonical ensembles, which will be compared to the simulation results.

Ensembles and Reference States. In principle, the basic building blocks are the polycations and polyanions. Because we will only consider the case of equal chain lengths, we can simplify matters by choosing 1:1 clusters and excess polycations instead. This assumes that rule I is obeyed at all times, which we have seen is a good approximation. The gain is that we need to consider fewer cluster types and we do not have to deal with the concentration of free polyanions, which becomes extremely small when polyanions are predominantly complexed to polycations.

Thus, we see the formation of a *m*:*n* cluster as the result of the following reaction:

$$(m-n)\{1{:}0\} + n\{1{:}1\} \rightarrow \{m{:}n\} \tag{8}$$

In the following, the 1:0 and 1:1 clusters will be collectively called unimers, to express their role as building blocks for larger clusters. The corresponding change in free energy (in units of k_BT) is

$$\begin{aligned}\Delta F_{m,n} &= \mu_{m,n} - (m-n)\mu_{1,0} - n\mu_{1,1} \\ &= \mu^\circ_{m,n} - (m-n)\mu^\circ_{1,0} - n\mu^\circ_{1,1} + \ln \frac{\rho_{m,n}}{\rho_{1,0}^{m-n}\,\rho_{1,1}^{n}}\end{aligned} \tag{9}$$

where $\mu_{m,n} = \mu^\circ_{m,n} + \ln \rho_{m,n}$ is the chemical potential of a *m*:*n* cluster with $\mu^\circ_{m,n}$ being the standard chemical potential and $\rho_{m,n}$ the number density, which implies that we ignore interactions between clusters. In a grand canonical ensemble, $\mu_{1,0}$ and $\mu_{1,1}$ are fixed and the equilibrium condition $\Delta F_{m,n} = 0$ leads to

$$\rho_{m,n} = \rho_{1,0}^{m-n}\,\rho_{1,1}^{n} \exp[(m-n)\mu^\circ_{1,0} + n\mu^\circ_{1,1} - \mu^\circ_{m,n}] \tag{10}$$

for all clusters.

For the canonical ensemble we have to consider separate states, which correspond to the different ways 1:0 and 1:1 clusters can be combined into complexes (or be left as free). Each state α, which is defined by listing the numbers, $N^\alpha_{m,n}$, of *m*:*n* clusters in the state, has a weight

$$\begin{aligned}W_\alpha &= \prod_{m,n} \frac{[V \exp(-\mu^\circ_{m,n})]^{N^\alpha_{m,n}}}{N^\alpha_{m,n}!} \\ &= \exp\{\sum_{m,n}[-N^\alpha_{m,n}(\mu^\circ_{m,n} - \ln V) - \ln(N^\alpha_{m,n}!)]\}\end{aligned} \tag{11}$$

where V is the volume of the system and appears here as another result of the approximation that there are no cluster−cluster interactions and every cluster is free to explore the whole volume as in an ideal gas. The factorial takes care of the fact that clusters are indistinguishable and reduces the overcounting implied in the volume term. The reason that we use the volume together with a factorial instead of just a concentration as in eq 9 is that we are dealing with small numbers of clusters and cannot rely on Stirling's approximation for large N, $\ln N! = N \ln N - N$,

to simplify the expression and give $\rho = N/V$. Finally, in the canonical ensemble, the average cluster concentration is obtained from

$$\rho_{m,n} = \frac{\langle N_{m,n} \rangle}{V} = \frac{\sum_{\alpha} N_{m,n}^{\alpha} W_{\alpha}}{V \sum_{\alpha} W_{\alpha}} \tag{12}$$

With concentrations given by eq 10 for the grand canonical ensemble and by eq 12 for the canonical ensemble, we can now calculate the cluster size probabilities $P_{m,n}$ according to

$$P_{m,n} = \frac{(m+n)\rho_{m,n}}{\sum_{m,n}(m+n)\rho_{m,n}} \tag{13}$$

Furthermore, for the sake of comparison with the simulations, the number densities in both ensembles are subject to the conservation laws with respect to total concentrations

$$\rho_{\text{pos}} \equiv \frac{N_{\text{pos}}}{V} = \sum_{m,n} m\rho_{m,n} \tag{14}$$

$$\rho_{\text{neg}} \equiv \frac{N_{\text{neg}}}{V} = \sum_{m,n} n\rho_{m,n} \tag{15}$$

This is automatically taken care of when we calculate the concentrations in a canonical ensemble (fixed N_{pos} and N_{neg}) by enumeration. For a grand canonical ensemble we have to find the concentrations $\rho_{1,0}$ and $\rho_{1,1}$ that via eq 10 give a distribution in accord with the conservation laws through an iterative calculation, and also use the condition that the largest possible cluster is a N_{pos}:N_{neg} cluster.

Standard Chemical Potentials. For the standard chemical potentials we will consider three energetic terms, and one volume (or inverse density) term according to

$$\mu^{\circ}_{m,n} = (m+n)C_{\text{bulk}} + (m+n)^{2/3}C_{\text{surf}} + \frac{(m-n)^2 C_{\text{el},1}}{(m+n)^{1/3}[1+(m+n)^{1/3}C_{\text{el},2}]} - (m-1)\ln(N_{\text{bead}}v_0) \tag{16}$$

The first term represents the net attractive interaction for chains in an infinite neutral cluster. The second is the reduction in this energy due to the lack of interactions on the surface of a finite cluster and it corresponds to rule III. The third term is the electrostatic interaction of a charged cluster ($m - n > 0$) and corresponds to rule II. It has the form of the free energy of a charged spherical shell obtained with the Debye−Hückel approximation.[31] In eq 16, $N_{\text{bead}}v_0$ is the volume available to a unimer in a complex and together with the unimer densities in eq 10 or the system volume in eq 11, the last term gives the probability that a unimer finds a cluster by volume ratio. Moreover, v_0 represents a unit of volume and makes the complete expressions dimensionless.

The most important information in eq 16 is the cluster size dependence of the different terms. This is what gives the general trends in the behavior, and the constants can simply be taken as adjustable parameters. For the sake of discussing the effects of the ensemble constraints in the simulations, we only need to find parameters that qualitatively reproduce the simulation results in the canonical ensemble. However, we have made an attempt to assign reasonable values to the constants before adjusting them, but it is not very important for the discussion of the results. We have therefore put these details in an appendix.

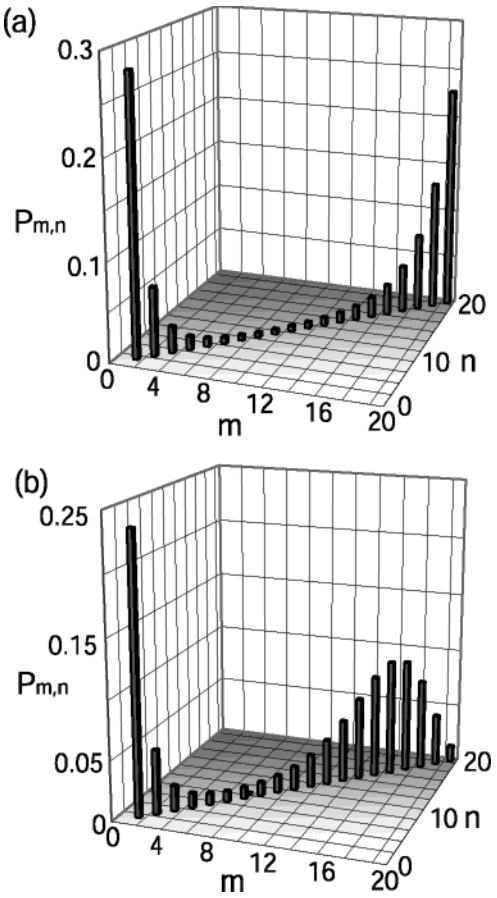

Figure 6. Cluster size probability distribution $P_{m,n}$ vs the number of polycations m and the number of polyanions n in polyion complexes obtained from free-energy calculations in (a) a grand canonical ensemble and (b) a canonical ensemble for system 20.

For a free polycation, which is one of our two types of unimers, we only have the electrostatic term, because there should be no correlation attraction when it is not interacting with a polyanion and we get

$$\mu^{\circ}_{1,0} = \frac{C_{\text{el},1}}{1 + C_{\text{el},2}} \tag{17}$$

We keep the expression for a charged sphere for consistency, although we would except a free polyion to be more rodlike than spherical. For the neutral 1:1 cluster, we do not have the electrostatic repulsion and

$$\mu^{\circ}_{1,1} = 2C_{\text{bulk}} + 2^{2/3}C_{\text{surf}} \tag{18}$$

Note that the bulk term is linear in $(m + n)$ and that all neutral complexes ($m = n$) therefore have the same "bulk energy" per polyion, which means that this term has no effect on the cluster size distribution when we only have neutral complexes, i.e., in systems with equal amounts of positive and negative polyions. With an excess of polycations, the bulk term reduces the amount of free polyions, because it does not exist for the 1:0 cluster, but the electrostatic repulsion also does this and the influence of the bulk term is generally insignificant.

Results and Discussion. Figure 6 shows the cluster distributions for system 20 obtained with the free-energy calculations

in a grand canonical and a canonical ensemble. This should be compared to the simulation results in Figure 3d.

The only energetic term that affects the distribution in this case is the surface term, which favors large clusters, whereas the entropic contribution prevents clustering and allows small clusters to persist. This balance between energy and entropy is clearly seen in the grand canonical case. Here the probability is increasing with size for the largest clusters, which mean that we could expect a phase separation in a larger system.

In the canonical ensemble, as in the simulations, the situation is different. There is still a tendency for bimodality, but the probabilities are declining instead of increasing for the largest clusters. This is a consequence of restricting the system to certain combinations of clusters, unlike in the grand canonical ensemble where each cluster is individually in equilibrium with a common reference state, namely a solution of the unimers, as described by eqs 8 and 10. The global equilibrium is also what we would have in a real solution, whereas the present results for the canonical ensemble shows a finite-size effect.

To illustrate the difference between the two ensembles, we look at the ratio of the weights of 20:20 and 19:19 clusters. In the grand canonical ensemble the ratio is $\rho_{20,20}/\rho_{19,19} = \rho_{1,1} \exp(\mu^\circ_{1,1} + \mu^\circ_{19,19} - \mu^\circ_{20,20}) = 1.6$, whereas in the canonical ensemble the corresponding ratio contains the weights of the state with just one 20:20 cluster and the state with a 1:1 and a 19:19 cluster, $W_{20:20}/W_{1:1+19:19} = \exp(\mu^\circ_{1,1} + \mu^\circ_{19,19} - \mu^\circ_{20,20})/V = 0.29$. In other words, the difference between the ratios lies in the equilibrium concentration $\rho_{1,1}$ in the grand canonical case, which corresponds to 5.6 unimers in the simulation box, compared to the factor $1/V$, which means one unimer in the box, for the canonical weights. From an entropic point, the canonical 19:19 lives in a 5.6 times too low unimer concentration and is as much less likely to combine into a 20:20 cluster.

Figure 7 shows the situation for system 18 and should be compared with Figure 3b. Once again we see that the canonical ensemble tends to push the distribution away from the largest clusters. Here we note that a 19:18 cluster in the canonical case requires the presence of a 1:0 cluster, which is strongly disfavored electrostatically. Thus, the larger complex is energetically penalized by association, apart from the entropic problem discussed above. The canonical constraints also shift the maximum of the distribution for clusters with one excess polycation from smaller to intermediate sizes.

We can understand the distributions in the grand canonical case in the following way. If we start from a system with equivalent amounts of polycation and polyanion charges, we will have a distribution like the one in Figure 6a with mainly very small and very large clusters, which shows the balance between entropy and surface energy. When we add two excess polycations, we can either put them together in the same cluster, or in separate clusters. We can also choose between very small and very large clusters, because if the electrostatic interactions are not very strong, we will retain some of the character of the original neutral distribution. If the excess polyions are paired, we are restricted to using the large clusters for electrostatic reasons. If we separate them, we can save entropy by having small charged clusters, which leaves free 1:1 clusters. Very small charged clusters are electrostatically disfavored, but we can compromise and the distribution peaks at a few sizes up from the minimal size.

Conclusions

On the basis of a simple spring-bead model representing a solution of oppositely charged polyions studied by Monte Carlo simulations, the formation of polyion complexes and the structure of the solution have been examined. In addition, a simple model based on a few free-energy terms was employed to further deepen our analysis.

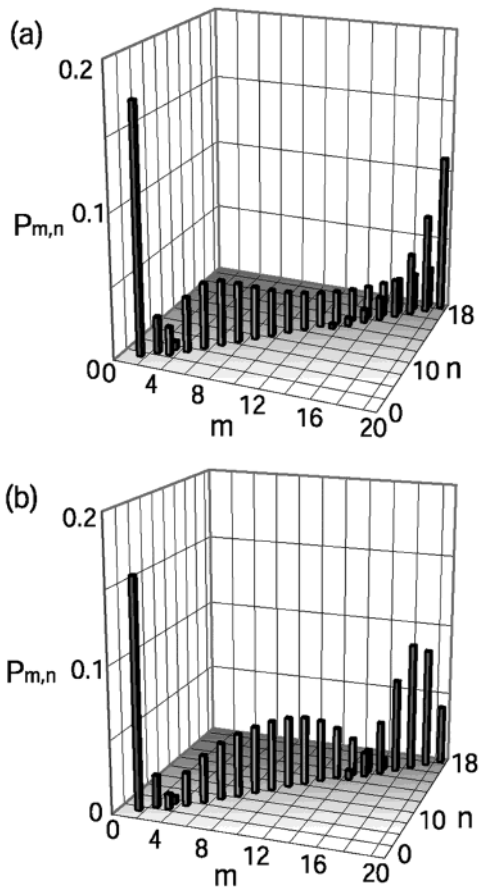

Figure 7. Cluster size probability distribution $P_{m,n}$ vs the number of polycations m and the number of polyanions n in polyion complexes obtained from free-energy calculations in (a) a grand canonical ensemble and (b) a canonical ensemble for system 18. Dark gray columns represent neutral clusters, light gray columns charged clusters with $m = n + 1$, and black columns charged clusters with $m = n + 2$.

In solutions of oppositely charged polyions with equal absolute charge, there is an increasing tendency to form large clusters as the excess of one kind of polyion is decreased. This tendency reaches a maximum near, but off, equivalent amounts of polycations and polyanions. At equivalent amounts, we obtained a bimodal distribution of small and large neutral clusters, in contrast to our previous study involving a smaller system, where we only had small clusters. The intermediate sized clusters are suppressed, because the system wants to minimize the total surface area of the clusters, whereas the smallest clusters survive for entropic reasons. With an excess of one kind of polyion, an additional driving force is a desire to spread the excess charges. When the excess is slight, larger charged clusters can be formed, which is preferred by the electrostatic repulsion among the excess polyions, but entropy still favors small clusters and a compromise is needed.

Also, when polycations and polyanions have different absolute charge, there is a strong tendency to form large complexes near or at equivalent amounts of positive and negative polyion charges. As the system departs from equivalence, complexes with a net charge are formed, which impedes the formation of large complexes. Moreover, as the length and charge asymmetry increases, an increasing fluctuation of the *number* of the small chains in the complexes appears. When the small polyions are

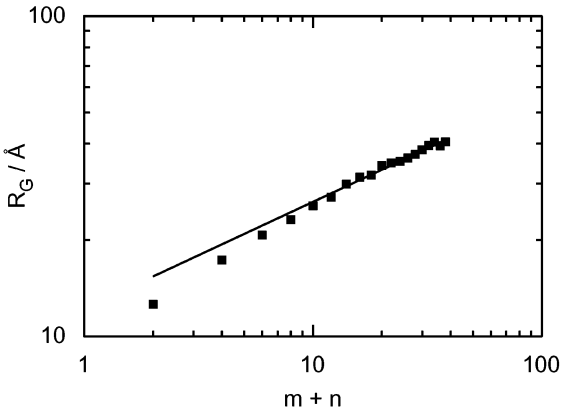

Figure 8. Radius of gyration R_G vs the number of polyions $m + n$ in a cluster from the simulation of system 20 (symbols) and a fit to that using eq 19 (line).

reduced to 5-mers, their electrostatic interaction with the longer polyions becomes insufficient to form large clusters and hence this system retains smaller separated clusters even at equivalent amounts of polyion charges.

The propensity for cluster formation was rationalized by four simple rules. For electrostatic reasons (I) a coexistence of oppositely charged clusters is unlikely and (II) excess charge is preferred to be located in clusters with low surface charge density and (III) large clusters are promoted to reduce the total cluster surface area, whereas from an entropic point of view (IV) many and consequently smaller clusters are preferred.

The elements behind these rules have also been put into a simple free-energy expression and cluster distributions have been calculated in grand canonical ensembles and canonical ensembles. The latter correspond to the simulations. The grand canonical results are expected to better reflect the equilibria in macroscopic systems (under the constraint of a maximum size for the clusters), whereas the canonical ensembles suffer from finite-size effects, which in the cases studied led to reduced probabilities for large clusters and shifted distributions.

Acknowledgment. Y.H. thanks T. Kawakatsu and F. Tanaka for a series of stimulating discussions. The work was supported by the Foundation of Strategic Research (SSF).

Appendix

In this appendix, we discuss the reasoning behind the terms in eq 16 and the assignment of parameter values. The basic idea was to get into the right ball park through reasonable approximations, but some fudging is necessary to mimic the simulation results in the canonical ensemble. Thus, the details of the approximations are not crucial and do not affect the conclusions.

The specific volume of a bead in a complex is denoted by v_0. Its inverse is the bead density $\rho_0 = 1/v_0 = 3/(4\pi\xi^3)$, where ξ is a characteristic length obtained from the assumption that the clusters are spherical with a radius that scales as

$$R_{m,n} = \xi[(m+n)N_{\text{bead}}]^{1/3} \tag{19}$$

To obtain a numerical estimate of the characteristic length, the radii of gyration of the clusters in system 20 have been plotted as a function of cluster size in Figure 8 and eq 19 has been fitted to the curve for the largest clusters. The result is $\xi = 4.5$ Å, which is a reasonable distance inside the cluster. The distance of closest approach between two beads is 4 Å. Furthermore, the agreement between simulation data and the form of eq 19 indicates that, to a good approximation, the volume of a complex grows linearly with the number of chains in the cluster.

The entropic term in eq 16 is obtained by considering the spherical cluster as a filled lattice that has the same fixed structure for all clusters of the same type; i.e, we ignore any fluctuations in shape and the possibility of 1:0 and 1:1 clusters exchanging sites (no mixing). There is only one way to fill such a lattice if the separate unimers are indistinguishable. Furthermore, one 1:1 cluster specifies the position of the cluster and represents the freedom of movement of the cluster as a whole. The other $(n - 1)$ 1:1 clusters and $(m - n)$ 1:0 clusters are confined to lattice sites, which have specific locations relative to the first 1:1 cluster. The size of a lattice site is taken to be $N_{\text{bead}}v_0$, which is the volume that a unimer (its center of mass) in a complex is free to explore. This is a compromise between two extremes: (i) close-packed beads and fixed chain conformations, which would imply a lattice volume corresponding to v_0, and (ii) an ideal gas of unimers inside a cluster, which would mean that they all had access to the volume $(m + n)N_{\text{bead}}v_0$.

As a rough estimate of the bulk term, we may picture the cluster as a dense solution of monovalently charged beads, and use the excess chemical potential given by the Debye−Hückel approximation. This approximation is not expected to hold for electrolytes at high concentrations and is expected to underestimate the correlations, but in the simulations, the interactions are somewhat reduced by the use of the screened Coulomb potential and the beads are connected into polyions and not free, which would also lessen correlation effects. Hence,

$$C_{\text{bulk}} = -N_{\text{bead}}\frac{l_B\kappa_{\text{cluster}}}{2} = -N_{\text{bead}}\frac{3^{1/2}l_B^{3/2}}{2\xi^{3/2}} \tag{20}$$

where $\kappa_{\text{cluster}} = (4\pi l_B\rho_0)^{1/2}$ is the Debye screening parameter obtained from the monomer density $\rho_0 = 3/(4\pi\xi^3)$ in a complex.

To approximate the surface term, we say that the beads in a shell of thickness ξ at the outer part of the spherical complex only experience interactions corresponding to half the excess chemical potential, which makes up the bulk term. From eq 19, we have that the volume of the spherical shell is $4\pi\xi^3[(m + n)N_{\text{bead}}]^{2/3}$, which is to be multiplied with ρ_0 to get the number of beads on the surface and the constant of the surface term becomes

$$C_{\text{surf}} = k_{\text{surf}}N_{\text{bead}}^{2/3}\frac{3^{3/2}l_B^{3/2}}{4\xi^{3/2}} \tag{21}$$

Here we have also introduced a fudge factor, k_{surf}, to be able to scale the surface term.

For the third term in the standard chemical potential, we use the electrostatic free energy of a sphere, with the net charge smeared on the surface and immersed in a solution of point ions, as obtained from the Debye−Hückel approximation,[31]

$$F_{\text{el}} = k_{\text{el}}\frac{(m-n)^2N_{\text{bead}}^2l_B}{2R_{m,n}(1+\kappa R_{m,n})} = k_{\text{el}}\frac{(m-n)^2N_{\text{bead}}^{5/3}l_B}{(n+m)^{1/3}2\xi[1+(n+m)^{1/3}N_{\text{bead}}^{1/3}\kappa\xi]} \tag{22}$$

where κ is the Debye screening parameter of the solution (the

value used in the simulations) and k_{el} is just a fudge factor. Thus, the constants in eq 16 are

$$C_{el,1} = k_{el}\frac{N_{bead}^{5/3} l_B}{2\xi} \tag{23}$$

and

$$C_{el,2} = N_{bead}^{1/3}\kappa\xi \tag{24}$$

With $N_{bead} = 20$, $l_B = 7.15$ Å, $\xi = 4.5$ Å, and a typical screening length $\kappa^{-1} = 11$ Å, we have $C_{bulk} = -35$, $C_{surf} = 19$, $C_{el,1} = 117$, $C_{el,2} = 1.1$, and $\rho_0 = 2.6 \times 10^{-3}$ Å^{-3}, without fudge factors. From comparison with system 20, we chose $k_{surf} = 0.25$ and system 18 led to the choice $k_{el} = 0.5$, which means that the results have been calculated with $C_{surf} = 4.8$ and $C_{el,1} = 59$.

References and Notes

(1) Bakeev, K. N.; Izumrudov, V. A.; Kuchanov, S. I.; Zezin, A. B.; Kabanov, V. A. *Macromolecules* **1992**, *25*, 4249.

(2) Kabanov, V. A. *Polym. Sci.* **1993**, *36*, 143.

(3) Kabanov, A. V.; Bronich, T. K.; Kabanov, V. A.; Yu, K.; Eisenberg, A. *Macromolecules* **1996**, *29*, 6797.

(4) Kabanov, V. A.; Zezin, A. B.; Rogacheva, V. B.; Gulyaeva, Z. G.; Zansochova, M. F.; Joosten, J. G. H.; Brackman, J. *Macromolecules* **1999**, *32*, 1904.

(5) Kabanov, V. A. Fundamentals of Polyelectrolyte Complexes in Solution and the Bulk. In *Multilayer Thin Films; Sequential Assembly of Nanocomposite Materials*; Decher, G., Schlenoff, J. B., Eds.; Wiley: New York, 2003.

(6) Pogodina, N. V.; Tsvetkov, N. V. *Macromolecules* **1997**, *30*, 4897.

(7) Ladam, G.; Schaad, P.; Voegel, J. C.; Schaaf, P.; Decher, G.; Cuisinier, F. *Langmuir* **2000**, *16*, 1249.

(8) Michel, E.; Gero, D. *Nano Lett.* **2001**, *1*, 45.

(9) *Fundamentals of Polyelectrolyte Complexes in Solution and the Bulk*; Decher, G., Schlenoff, J. B., Eds.; Wiley: New York, 2003.

(10) Dautzenberg, H. *Macromolecules* **1997**, *30*, 7810.

(11) Christos, G. A.; Carnie, S. L. *J. Chem. Phys.* **1990**, *92*, 7661.

(12) Stevens, M. J.; Kremer, K. *Macromolecules* **1993**, *26*, 4717.

(13) Stevens, M. J.; Kremer, K. *Phys. Rev. Lett.* **1993**, *71*, 2228.

(14) Stevens, M. J.; Kremer, K. *J. Chem. Phys.* **1995**, *103*, 1669.

(15) Stevens, M. J.; Kremer, K. *J. Phys. II Fr.* **1996**, *6*, 1607.

(16) Valleau, J. P. *J. Chem. Phys.* **1989**, *129*, 163.

(17) Christos, G. A.; Carnie, S. L. *Chem. Phys. Lett.* **1990**, *172*, 249.

(18) Woodward, C. E.; Jönsson, B. *J. Chem. Phys.* **1991**, *155*, 207.

(19) Ullner, M.; Woodward, C. E. *Macromolecules* **2000**, *33*, 7144.

(20) Borue, V. Y.; Erukhimovich, I. Y. *Macromolecules* **1990**, *23*, 2625.

(21) Srivastava, D.; Muthukumar, M. *Macromolecules* **1994**, *27*, 1461.

(22) Winkler, R. G.; Steinhauser, M. O.; Reineker, P. *Phys. Rev. E* **2002**, *66*, 021802.

(23) Dias, R. S.; Pais, A. A. C. C.; Miguel, M. G.; Lindman, B. *J. Chem. Phys.* **2003**, *119*, 8150.

(24) Messina, R.; Holm, C.; Kremer, K. *Langmuir* **2003**, *19*, 4473.

(25) Messina, R. *Macromolecules*, in press.

(26) Hayashi, Y.; Ullner, M.; Linse, P. *J. Chem. Phys.* **2002**, *116*, 6836.

(27) Hayashi, Y.; Ullner, M.; Linse, P. *J. Phys. Chem. B* **2003**, *107*, 8198.

(28) Metropolis, N.; Rosenbluth, A. W.; Rosenbluth, M. N.; Teller, A. H.; Teller, E. *J. Chem. Phys.* **1953**, *21*, 1087.

(29) Allen, M. P.; Tildesley, D. J. *Computer Simulation of Liquids*; Oxford: New York, 1987.

(30) Linse, P. *MOLSIM*, 3.0 ed.; Lund University: Sweden, 2000.

(31) Hill, T. L. *Arch. Biochem. Biophys.* **1955**, *57*, 229.